PERGAMON

International Journal of Solids and Structures 39 (2002) 673–687

INTERNATIONAL JOURNAL OF SOLIDS and STRUCTURES

www.elsevier.com/locate/ijsolstr

Three-dimensional vibration analysis of cantilevered and completely free isosceles triangular plates

Y.K. Cheung [a,*], D. Zhou [b]

[a] *Department of Civil Engineering, The University of Hong Kong, Pokfulam Road, Hong Kong*

[b] *Department of Applied Mechanics and Civil Engineering, Nanjing University of Science and Technology, Nanjing 210014, China*

Received 10 August 2000; received in revised form 4 August 2001

Abstract

The free vibration of cantilevered and completely free isosceles triangular plates based on exact three-dimensional elasticity theory is investigated. The actual plate domain is first mapped onto a basic cubic domain. Then the Ritz method is applied to derive the eigenfrequency equation from the strain energy and the kinetic energy of the plate. A set of Chebyshev polynomial series multiplied by a boundary function chosen to satisfy the essential geometry boundary conditions of the plate is developed as the admissible functions of each displacement component. The convergence and comparison studies show that rather accurate results can be obtained by using this approach. The effects of thickness-to-width ratio and apex angle on eigenfrequencies of the plates are studied in detail. Sets of valuable results are presented, which may serve as the benchmark values for future numerical techniques in thick plate vibration analysis. Data for the completely free isosceles triangular plates are presented for the first time.

Keywords: Three-dimensional vibration; Ritz method; Isosceles triangular plate; Thick plate; Chebyshev polynomial; Eigenfrequencies

1. Introduction

Triangular plates can be found as basic structural elements in civil, mechanical, aircraft and marine engineering. In some cases the plates have to bear the dynamic loads, and therefore, to understand their dynamic characteristics is very important for designers. By making a careful search of the literature, the authors found that much of the triangular plate vibration analyses are based on the two-dimensional classical thin plate theory. Since no exact solution has been presented for this problem, numerical approximation approaches such as the finite element method (Batoz et al., 1980), finite difference method (Cox and Klein, 1995), superposition method (Gorman, 1989a,b), and Rayleigh–Ritz method (Kim and Dickinson, 1990; Lam et al., 1990) have to be used.

It is well known that the classical thin plate theory (Timoshenko and Woinowsky-Krieger, 1959) has not taken into account the effect of transverse shear deformation and rotary inertia. However, the shear deformation becomes increasingly important as the thickness–span ratio increases. Also, even for thinner

* Corresponding author. Tel.: +852-2859-2668; fax: +852-2559-5337.
E-mail address: hreccyk@hkucc.hku.hk (Y.K. Cheung).

0020-7683/02/$ - see front matter
PII: S0020-7683(01)00196-2

plates this effect of rotary inertia should be considered when higher vibration modes are required. Mindlin (1951) proposed the so-called first-order shear deformation theory by assuming a constant shear strain distribution through the plate thickness. A shear correction factor is then introduced to compensate the errors resulting from the approximation made on the non-uniform shear strain distribution. More accurate results than those from the classical plate theory can be obtained, especially for moderately thick plates. Recently, Kitipornchai et al. (1993) and Karunasena et al. (1996) studied the free vibration of isosceles triangular Mindlin plates and cantilevered arbitrary triangular Mindlin plates by using the Rayleigh–Ritz method. Moreover, McGee and Butalia (1992) used the finite element method to compute the eigenfrequencies of cantilevered skewed triangular thick plates, based on a higher order shear deformation theory. It is obvious that Mindlin plate theory cannot show the symmetric modes (in-plane modes) in the thickness direction. However, for many of moderately thick triangular plates (in general, the thickness–span ratio more than 0.1), the first one or two eigenfrequencies of the symmetric modes in the thickness direction are still in the scope of the low-order eigenfrequencies (first several eigenfrequencies) of the plates. Therefore, to obtain a complete understanding on the dynamic characteristic of thick triangular plates, three-dimensional elasticity theory must be employed, even for moderately thick triangular plates.

Up to date, the research on three-dimensional vibration analysis of triangular plates has been very limited and only two references concerned with this problem have been found. McGee and Giaimo (1992) studied the three-dimensional vibration of cantilevered right triangular plates using general algebraic polynomials as admissible functions in the Ritz method. Liew et al. (1994) studied the three-dimensional vibration of cantilevered skewed trapezoids by using one- and two-dimensional orthogonal polynomial functions as admissible functions. Some numerical results about cantilevered triangular plates are given. Both these investigations are focused on the cantilevered triangular plates. The available data are far from enough to satisfy the need of engineering application and research work. No result about triangular plates with other boundary conditions can be obtained from the literature. Considering the wide applications of isosceles triangular plates in various engineering, it is important to present the accurate three-dimensional vibration analysis in detail. In this paper, the three-dimensional elasticity solutions to vibration of cantilevered and completely free isosceles triangular plates are studied by the Ritz method. By mapping the actual plate domain onto a basic cubic domain, a set of Chebyshev polynomials multiplied by a boundary function is developed as the admissible functions of each displacement component. The boundary function is chosen such that the admissible functions can satisfy the essential geometric boundary conditions of the plate. It should be mentioned that the present method is suitable for the vibration analysis of arbitrary triangular plates. However only the isosceles triangular plates are discussed as the typical example in this paper. It is convenient for our analysis that isosceles triangular plates have two symmetric planes: the mid-plane of the plate and the plane orthogonal to the mid-plane and bisecting the apex angle of the plate. Therefore, the vibration modes of isosceles triangular plates can be divided into four distinct symmetry classes. They are, respectively, symmetric–symmetric modes (SS); symmetric (about the mid-plane)–antisymmetric (about the bisecting-plane) modes (SA); antisymmetric–symmetric modes (AS) and antisymmetric–antisymmetric modes (AA). This classification has two apparent advantages. One is the size of the determinant from the resulting eigenfrequency equation is greatly reduced. The other is the effect of thickness–span ratio on the symmetric modes about the mid-plane can be clearly shown, which can be neither obtained by the classical plate theory nor the Mindlin plate theory.

2. Theoretical formulation

Consider an isosceles triangular plate with width a, thickness t and apex angle α as shown in Fig. 1(a). The strain energy $\overline{V}$ and the kinetic energy $\overline{T}$ of a three-dimensional elastic body undergoing free vibration are given by the volume integrals

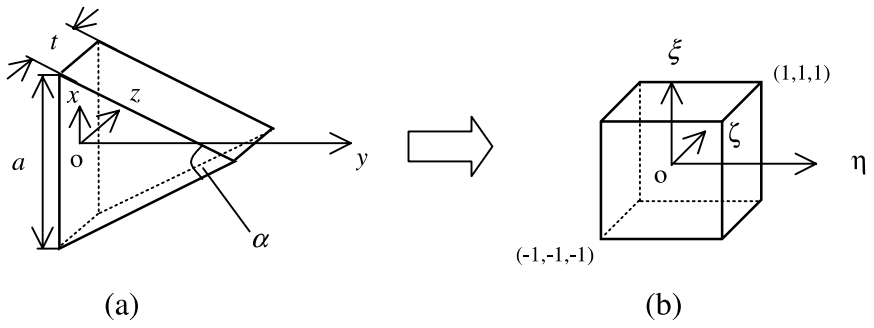

Fig. 1. Domain transformation: (a) isosceles triangular plate; (b) basic cubic domain.

$$\begin{aligned}\overline{V} &= (1/2)\int\int\int [\lambda(\varepsilon_x+\varepsilon_y+\varepsilon_z)^2 + 2G(\varepsilon_x^2+\varepsilon_y^2+\varepsilon_z^2) + G(\gamma_{xy}^2+\gamma_{yz}^2+\gamma_{zx}^2)]\,\mathrm{d}x\,\mathrm{d}y\,\mathrm{d}z,\\ \overline{T} &= (\rho/2)\int\int\int (\dot{u}+\dot{v}+\dot{w})\,\mathrm{d}x\,\mathrm{d}y\,\mathrm{d}z,\end{aligned} \tag{1}$$

where ρ is a constant mass per unit volume; $u = u(x,y,z)$, $v = v(x,y,z)$ and $w = w(x,y,z)$ are displacement components in the x, y and z directions, respectively; $\dot{u}$, $\dot{v}$ and $\dot{w}$ are the corresponding velocity components. λ and G are the Lame constants for a homogeneous and isotropic material, which are expressed in terms of Young's modulus E and the Poisson's ratio v by

$$\lambda = vE/[(1+v)(1-2v)], \qquad G = E/[2(1+v)]. \tag{2}$$

In Eq. (1), the linear strain–displacement relations are given by

$$\begin{aligned}&\varepsilon_x = \partial u/\partial x, \qquad \varepsilon_y = \partial v/\partial y, \qquad \varepsilon_z = \partial w/\partial z,\\ &\gamma_{xy} = \partial v/\partial x + \partial u/\partial y, \qquad \gamma_{yz} = \partial w/\partial y + \partial v/\partial z, \qquad \gamma_{zx} = \partial u/\partial z + \partial w/\partial x.\end{aligned} \tag{3}$$

For free vibrations, the displacement components of the three-dimensional elastic body may be expressed as

$$u = U(x,y,z)\mathrm{e}^{\mathrm{i}\omega t}, \qquad v = V(x,y,z)\mathrm{e}^{\mathrm{i}\omega t}, \qquad w = W(x,y,z)\mathrm{e}^{\mathrm{i}\omega t}, \tag{4}$$

where ω is the circular eigenfrequency of vibration.

Substituting Eqs. (3) and (4) into Eq. (1), the maximum strain energy $\overline{V}_{\max}$ and the maximum kinetic energy $\overline{T}_{\max}$ of the plate are, respectively, expressed as

$$\begin{aligned}\overline{V}_{\max} &= (1/2)\int\int\int [\lambda\overline{V}_1 + G(\overline{V}_2+\overline{V}_3)]\,\mathrm{d}x\,\mathrm{d}y\,\mathrm{d}z,\\ \overline{T}_{\max} &= (1/2)\rho\omega^2\int\int\int (U^2+V^2+W^2)\,\mathrm{d}x\,\mathrm{d}y\,\mathrm{d}z,\end{aligned} \tag{5}$$

in which,

$$\begin{aligned}\overline{V}_1 &= \partial U/\partial x + \partial V/\partial y + \partial W/\partial z,\\ \overline{V}_2 &= 2(\partial U/\partial x)^2 + 2(\partial V/\partial y)^2 + 2(\partial W/\partial z)^2,\\ \overline{V}_3 &= (\partial U/\partial y + \partial V/\partial x)^2 + (\partial V/\partial z + \partial W/\partial y)^2 + (\partial W/\partial x + \partial U/\partial z)^2.\end{aligned} \tag{6}$$

The Lagrangian energy functional L is given as

$$L = \overline{T}_{\max} - \overline{V}_{\max}. \tag{7}$$

For simplicity, the actual isosceles triangular prism domain is mapped onto a basic cubic domain, as shown in Fig. 1(b), using the following co-ordinate transformation

$$x = a\xi(1-\eta)/4, \qquad y = a(1+\cos\alpha)(1+\eta)/(4\sin\alpha), \qquad z = t\zeta/2. \tag{8}$$

Applying the chain rule of differentiation, the relation of the first derivative in the two co-ordinate systems can be expressed as

$$\begin{Bmatrix} \frac{\partial()}{\partial x} \\ \frac{\partial()}{\partial y} \end{Bmatrix} = \boldsymbol{J}^{-1} \begin{Bmatrix} \frac{\partial()}{\partial \xi} \\ \frac{\partial()}{\partial \eta} \end{Bmatrix}, \qquad \frac{\partial()}{\partial z} = \frac{t}{2}\frac{\partial()}{\partial \zeta}, \tag{9}$$

where

$$\boldsymbol{J} = \begin{bmatrix} \frac{\partial x}{\partial \xi} & \frac{\partial y}{\partial \xi} \\ \frac{\partial x}{\partial \eta} & \frac{\partial y}{\partial \eta} \end{bmatrix} = \frac{a}{4}\begin{bmatrix} 1-\eta & 0 \\ -\xi & (1+\cos\alpha)/\sin\alpha \end{bmatrix}, \tag{10}$$

in which, $\boldsymbol{J}$ denotes the Jacobian matrix of the geometrical mapping. Eqs. (9) and (10) will be used later to transform the x–y–z domain integrals in Eqs. (1) and (2) into ξ–η–ζ domain integrals.

The displacement functions $U(x,y,z) = U(\xi,\eta,\zeta)$, $V(x,y,z) = V(\xi,\eta,\zeta)$ and $W(x,y,z) = W(\xi,\eta,\zeta)$ are approximately expressed in terms of a finite series as

$$\begin{aligned} U(\xi,\eta,\zeta) &= f_u(\xi,\eta,\zeta)\sum_{i=1}^{I}\sum_{j=1}^{J}\sum_{k=1}^{K} A_{ijk}F_i(\xi)F_j(\eta)F_k(\zeta), \\ V(\xi,\eta,\zeta) &= f_v(\xi,\eta,\zeta)\sum_{l=1}^{L}\sum_{m=1}^{M}\sum_{n=1}^{N} B_{lmn}F_l(\xi)F_m(\eta)F_n(\zeta), \\ W(\xi,\eta,\zeta) &= f_w(\xi,\eta,\zeta)\sum_{p=1}^{P}\sum_{q=1}^{Q}\sum_{r=1}^{R} C_{pqr}F_p(\xi)F_q(\eta)F_r(\zeta), \end{aligned} \tag{11}$$

where A_{ijk}, B_{lmn} and C_{pqr} are undetermined coefficients, $f_u(\xi,\eta,\zeta)$, $f_v(\xi,\eta,\zeta)$ and $f_w(\xi,\eta,\zeta)$ are the boundary functions while all the series functions have an identical form of formulation: $F_s(\chi)$ ($s = i,j,k,l,m,n,p,q,r$ and $\chi = \xi,\eta,\zeta$) which are a set of Chebyshev polynomials defined in interval $[-1,1]$, expressed by

$$F_s(\chi) = \cos[(s-1)\arccos(\chi)], \quad s = 1,2,3,\ldots \tag{12}$$

It should be noted that selecting Chebyshev polynomial series as the admissible functions of each displacement component has two distinct advantages (Fox and Parker, 1968). One is that $F_s(\chi)$ ($s = 1,2,3,\ldots$) is a set of complete and orthogonal series in interval $[-1,1]$, which has more rapid convergence and better numerical stability in computation than other polynomial series such as the Taylor series. The other is that $F_s(\chi)$ ($s = 1,2,3,\ldots$) can be expressed in a simple and unified form of cosine function, which reduces the coding effort. The first five Chebyshev polynomials are given in Fig. 2.

In using the Ritz method, the stress boundary conditions of the plates need not be satisfied in advance, however, the geometric boundary conditions should be satisfied exactly. Therefore, the boundary functions for cantilevered plates are given by

$$f_u(\xi,\eta,\zeta) = f_v(\xi,\eta,\zeta) = f_w(\xi,\eta,\zeta) = 1+\xi, \tag{13}$$

and the boundary functions for completely free plates are given by

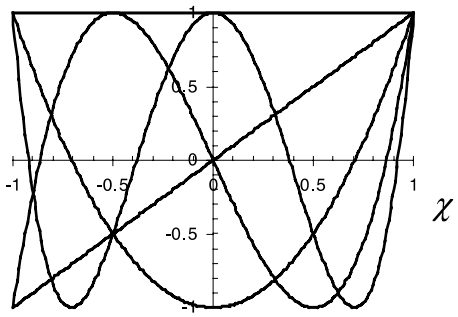

Fig. 2. The first five terms of Chebyshev polynomial series $F_s(\chi)$ $(s = 1, 2, 3, 4, 5)$.

$$f_u(\xi,\eta,\zeta) = f_v(\xi,\eta,\zeta) = f_w(\xi,\eta,\zeta) = 1. \tag{14}$$

Substituting Eqs. (7)–(9) into Eqs. (5)–(7), the Lagrangian functional L can be expressed in terms of the co-ordinate system ξ–η–ζ as follows

$$\begin{aligned} L = {} & (t/4)\rho\omega^2 \int_{-1}^{1}\int_{-1}^{1}\int_{-1}^{1}(U^2+V^2+W^2)|\boldsymbol{J}|\,\mathrm{d}\xi\,\mathrm{d}\eta\,\mathrm{d}\zeta \\ & - (t/4)\int_{-1}^{1}\int_{-1}^{1}\int_{-1}^{1}[\lambda\overline{V}_1 + G(\overline{V}_2+\overline{V}_3)]|\boldsymbol{J}|\,\mathrm{d}\xi\,\mathrm{d}\eta\,\mathrm{d}\zeta, \end{aligned} \tag{15}$$

where $|\boldsymbol{J}| = a^2(1-\eta)(1+\cos\alpha)/(16\sin\alpha)$ is the determinant of the Jacobian matrix $\boldsymbol{J}$.

Substituting Eq. (11) into the L expression, and minimizing L with respect to the undetermined coefficients A_{ijk}, B_{lmn} and C_{pqr}, a set of eigenfrequency equations is derived, which can be written in matrix form as

$$\left(\begin{bmatrix} [K_{uu}] & [K_{uv}] & [K_{uw}] \\ [K_{uv}]^{\mathrm{T}} & [K_{vv}] & [K_{vw}] \\ [K_{uw}]^{\mathrm{T}} & [K_{vw}]^{\mathrm{T}} & [K_{ww}] \end{bmatrix} - \Omega^2 \begin{bmatrix} M_{uu} & 0 & 0 \\ 0 & M_{vv} & 0 \\ 0 & 0 & M_{ww} \end{bmatrix} \right) \begin{Bmatrix} \{A\} \\ \{B\} \\ \{C\} \end{Bmatrix} = \begin{Bmatrix} \{0\} \\ \{0\} \\ \{0\} \end{Bmatrix}, \tag{16}$$

in which $\Omega = \omega a(\rho/E)^{1/2}$, $[K_{ij}]$ and $[M_{ii}]$ $(i,j = u,v,w)$ are the sub-stiffness matrices and the diagonal sub-mass matrices. $\{A\}$, $\{B\}$ and $\{C\}$ are the column vectors of the unknown coefficients which are expressed in the following forms

$$\{A\} = \begin{Bmatrix} A_{111} \\ A_{112} \\ \vdots \\ A_{11K} \\ A_{121} \\ \vdots \\ A_{12K} \\ \vdots \\ A_{1JK} \\ \vdots \\ A_{IJK} \end{Bmatrix}, \qquad \{B\} = \begin{Bmatrix} B_{111} \\ B_{112} \\ \vdots \\ B_{11N} \\ B_{121} \\ \vdots \\ B_{12N} \\ \vdots \\ B_{1MN} \\ \vdots \\ A_{LMN} \end{Bmatrix}, \qquad \{C\} = \begin{Bmatrix} C_{111} \\ C_{112} \\ \vdots \\ C_{11R} \\ C_{121} \\ \vdots \\ C_{12R} \\ \vdots \\ C_{1QR} \\ \vdots \\ C_{PQR} \end{Bmatrix}. \tag{17}$$

The expressions of the various elements in every sub-matrices $[K_{ij}]$ and $[M_{ii}]$ $(i,j=u,v,w)$ are given by

$$[K_{uu}]=\frac{(1-v)(1+\cos\alpha)}{(1-2v)\sin\alpha}E^{110}_{uiu\bar{i}}G^{00-1}_{uju\bar{j}}H^{00}_{uku\bar{k}}+\frac{\sin\alpha}{2(1+\cos\alpha)}(E^{112}_{uiu\bar{i}}G^{00-1}_{uju\bar{j}}+E^{00}_{uiu\bar{i}}G^{111}_{uju\bar{j}}+E^{101}_{uiu\bar{i}}G^{010}_{uju\bar{j}}$$
$$+E^{011}_{uiu\bar{i}}G^{100}_{uju\bar{j}})H^{00}_{uku\bar{k}}+\frac{1+\cos\alpha}{8\gamma^2\sin\alpha}E^{000}_{uiu\bar{i}}G^{001}_{uju\bar{j}}H^{00}_{uku\bar{k}},$$

$$[K_{vv}]=\frac{(1-v)\sin\alpha}{(1-2v)(1+\cos\alpha)}(E^{112}_{vlv\bar{l}}G^{00-1}_{vmv\bar{m}}+E^{000}_{vlv\bar{l}}G^{111}_{vmv\bar{m}}+E^{101}_{vlv\bar{l}}G^{010}_{vmv\bar{m}}+E^{011}_{vlv\bar{l}}G^{100}_{vmv\bar{m}})H^{00}_{vnv\bar{n}}$$
$$+\frac{1+\cos\alpha}{8\gamma^2\sin\alpha}E^{000}_{vlv\bar{l}}G^{001}_{vmv\bar{m}}H^{11}_{vnv\bar{n}}+\frac{1+\cos\alpha}{2\sin\alpha}E^{110}_{vlv\bar{l}}G^{00-1}_{vmv\bar{m}}H^{00}_{vnv\bar{n}},$$

$$[K_{ww}]=\frac{(1-v)(1+\cos\alpha)}{4(1-2v)\sin\alpha}E^{000}_{wpw\bar{p}}G^{001}_{wqw\bar{q}}H^{11}_{wrw\bar{r}}+\frac{\sin\alpha}{2(1+\cos\alpha)}(E^{112}_{wpw\bar{p}}G^{00-1}_{wqw\bar{q}}+E^{000}_{wpw\bar{p}}G^{111}_{wqw\bar{q}}$$
$$+E^{101}_{wpw\bar{p}}G^{010}_{wqw\bar{q}}+E^{011}_{wpw\bar{p}}G^{100}_{wqw\bar{q}})H^{00}_{wrw\bar{r}}+\frac{1+\cos\alpha}{2\sin\alpha}E^{110}_{wpw\bar{p}}G^{00-1}_{wqw\bar{q}}H^{00}_{wrw\bar{r}},$$

$$[K_{uv}]=\frac{v}{1-2v}(E^{111}_{uiv\bar{l}}G^{00-1}_{ujv\bar{m}}+E^{100}_{uiv\bar{l}}G^{010}_{ujv\bar{m}})H^{00}_{ukv\bar{n}}+\frac{1}{2}(E^{111}_{uiv\bar{l}}G^{00-1}_{ujv\bar{m}}+E^{010}_{uiv\bar{l}}G^{100}_{ujv\bar{m}})H^{00}_{ukv\bar{n}},$$

$$[K_{uw}]=\frac{(1+\cos\alpha)}{4\gamma\sin\alpha}\left(\frac{2v}{1-2v}E^{100}_{uiw\bar{p}}G^{000}_{ujw\bar{q}}H^{01}_{ukw\bar{r}}+E^{010}_{uiw\bar{p}}G^{000}_{ujw\bar{q}}H^{10}_{ukw\bar{r}}\right),$$

$$[K_{vw}]=\frac{1}{2\gamma^2}\left[\frac{2v}{1-2v}(E^{101}_{vlw\bar{p}}G^{000}_{vmw\bar{q}}+E^{000}_{vlw\bar{p}}G^{101}_{vmw\bar{q}})H^{01}_{vnw\bar{r}}+(E^{011}_{vlw\bar{p}}G^{000}_{vmw\bar{q}}+E^{000}_{vlw\bar{p}}G^{011}_{vmw\bar{q}})H^{10}_{vnw\bar{r}}\right],$$

$$[M_{uu}]=\frac{(1+v)(1+\cos\alpha)}{32\sin\alpha}E^{000}_{uiu\bar{i}}G^{001}_{uju\bar{j}}H^{00}_{uku\bar{k}},$$

$$[M_{vv}]=\frac{(1+v)(1+\cos\alpha)}{32\sin\alpha}E^{000}_{vlv\bar{l}}G^{001}_{vmv\bar{m}}H^{00}_{vnv\bar{n}},$$

$$[M_{ww}]=\frac{(1+v)(1+\cos\alpha)}{32\sin\alpha}E^{000}_{vpv\bar{p}}G^{001}_{vqv\bar{q}}H^{00}_{wrw\bar{r}}$$

$$E^{\theta\sigma\varsigma}_{\alpha s\beta\bar{s}}=\int_{-1}^{1}[d^{\theta}F_s(\xi)/\mathrm{d}\xi^{\theta}][d^{\sigma}F_{\bar{s}}(\xi)/\mathrm{d}\xi^{\sigma}]\xi^{\varsigma}\,\mathrm{d}\xi,$$

$$G^{\theta\sigma\tau}_{\alpha s\beta\bar{s}}=\int_{-1}^{1}[d^{\theta}\overline{F}_s(\eta)/\mathrm{d}\eta^{\theta}][d^{\sigma}\overline{F}_{\bar{s}}(\eta)/\mathrm{d}\eta^{\sigma}](1-\eta)^{\tau}\,\mathrm{d}\eta,$$

$$H^{\theta\sigma}_{\alpha s\beta\bar{s}}=\int_{-1}^{1}[d^{\theta}F_s(\zeta)/\mathrm{d}\zeta^{\theta}][d^{\sigma}F_{\bar{s}}(\zeta)/\mathrm{d}\zeta^{\sigma}]\mathrm{d}\zeta, \tag{18}$$

in which,

$$\theta,\sigma=0,1,\qquad \varsigma=0,1,2,\qquad \tau=-1,0,1,\qquad \alpha,\beta=u,v,w,\qquad s=i,j,k,l,m,n,p,q,r,$$
$$\bar{s}=\bar{i},\bar{j},\bar{k},\bar{l},\bar{m},\bar{n},\bar{p},\bar{q},\bar{r},\qquad \gamma=t/a,\qquad \overline{F}_s(\eta)=(1+\eta)^{\delta}F_s(\eta), \tag{19}$$

for the cantilevered plates $\delta=1$, and for the completely free plates $\delta=0$.

It is obvious that for both cantilevered isosceles triangular plates and completely free isosceles triangular plates, two symmetric planes exist. One is the x–y plane ($z=0$: the mid-plane of the plate) and the other is the y–z plane ($x=0$: the bisecting plane). In such a case, one should take advantage of the symmetry to reduce the size of the eigenfrequency equation. For the symmetric modes about x–y plane, one should take k,$n=1,3,5,\ldots$, $r=2,4,6,\ldots$ For the antisymmetric modes about x–y plane, one should take k, $n=2,4,6,\ldots$, $r=1,3,5,\ldots$ For the symmetric modes about y–z plane, one should take $i=2,4,6,\ldots$, l, $p=1,3,5,\ldots$ While for the antisymmetric modes about y–z plane, one should take $i=1,3,5,\ldots$, l, $p=2,4,6,\ldots$ Correspondingly, the vibration modes of the plates can also be divided into four distinct

categories. They are, respectively, SS modes; SA (about the mid-plane x–y)–(about the bisecting-plane y–z) modes; AS modes and AA modes. Each of these categories can be separately investigated. A non-trivial solution is obtained by setting the determinant of the coefficient matrix of equation (16) equal to zero. Roots of the determinant are the square of the non-dimensional eigenfrequencies (eigenvalues). Mode shapes (eigenfunctions) are determined by back-substitution of the eigenvalues, one-by-one, in the usual manner. All computations are performed in double precision (16 significant figures) on a microcomputer. The integrals in Eq. (18) are numerically evaluated by the piecewise Gauss quadrature with 24 points.

3. Convergence and comparison studies

As it is well known, eigenfrequencies by the Ritz method converge in the manner of upper bounds to the exact values. These upper bounds could be improved by increasing the numbers of terms of the admissible functions in the computation. To demonstrate the accuracy and convergence of the method, the numerical results of AS modes for completely free equilateral triangular plates are presented in Table 1 with respect to the numbers of terms of the Chebyshev polynomials. Three different thickness-to-width ratios $\gamma = 0.05$, $\gamma = 0.15$ and $\gamma = 0.45$ are considered. For convenience in comparing with available results, an eigenfrequency parameter λ is defined as

Table 1
The convergence study of eigenfrequencies of AS modes for completely free equilateral triangular plates

Terms	λ_1	λ_2	λ_3	λ_4	λ_5	λ_6
$\gamma = 0.05$						
$3 \times 6 \times 3$	5.4031	5.5848	13.368	18.055	32.974	34.706
$4 \times 8 \times 2$	5.3500	5.5439	12.891	17.453	24.614	24.769
$4 \times 8 \times 4$	5.3500	5.5439	12.891	17.453	24.613	24.765
$5 \times 10 \times 2$	5.3467	5.5400	12.871	17.334	23.734	23.815
$5 \times 10 \times 4$	5.3467	5.5400	12.871	17.334	23.733	23.814
$6 \times 12 \times 2$	5.3458	5.5392	12.868	17.324	23.690	23.784
$6 \times 12 \times 4$	5.3458	5.5392	12.868	17.323	23.689	23.783
$8 \times 16 \times 2$	5.3456	5.5391	12.868	17.321	23.686	23.781
$9 \times 18 \times 2$	5.3456	5.5391	12.868	17.321	23.686	23.781
$\gamma = 0.15$						
$3 \times 6 \times 3$	4.8427	4.8532	10.513	13.704	19.823	21.848
$4 \times 8 \times 2$	4.8335	4.8355	10.354	13.414	16.767	17.673
$4 \times 8 \times 3$	4.8330	4.8350	10.350	13.405	16.750	17.649
$4 \times 8 \times 6$	4.8330	4.8350	10.350	13.405	16.749	17.649
$5 \times 10 \times 2$	4.8331	4.8352	10.347	13.389	16.534	17.384
$5 \times 10 \times 3$	4.8326	4.8347	10.343	13.382	16.521	17.367
$5 \times 10 \times 6$	4.8326	4.8347	10.343	13.382	16.521	17.367
$6 \times 12 \times 3$	4.8325	4.8347	10.343	13.381	16.515	17.360
$7 \times 14 \times 3$	4.8325	4.8347	10.343	13.381	16.515	17.360
$\gamma = 0.45$						
$3 \times 6 \times 4$	2.8866	3.2029	4.6498	5.2150	6.6944	6.9614
$4 \times 8 \times 3$	2.8852	3.1971	4.6390	5.1955	6.6039	6.8034
$4 \times 8 \times 4$	2.8851	3.1970	4.6387	5.1952	6.6032	6.8029
$4 \times 8 \times 6$	2.8851	3.1970	4.6387	5.1952	6.6032	6.8028
$5 \times 10 \times 3$	2.8852	3.1970	4.6384	5.1945	6.5999	6.7954
$5 \times 10 \times 4$	2.8851	3.1970	4.6381	5.1943	6.5993	6.7950
$5 \times 10 \times 6$	2.8851	3.1970	4.6381	5.1943	6.5993	6.7950
$6 \times 12 \times 4$	2.8851	3.1970	4.6381	5.1943	6.5993	6.7950

Table 2
The comparison study of eigenfrequencies for the cantilevered isosceles triangular plate with $\gamma = 0.1$, $\alpha = 53.13°$ using three-dimensional elasticity theory in the Ritz method

Terms	Determinent size	λ_1^{AS}	λ_2^{AA}	λ_3^{AS}	λ_4^{SA}	λ_5^{AS}	λ_6^{AA}
$3 \times 6 \times 2$	108	1.0562	4.2419	4.3304	5.7395	9.8630	10.446
$4 \times 8 \times 2$	192	1.0530	4.2228	4.3174	5.7361	9.7123	10.270
$5 \times 10 \times 2$	300	1.0518	4.2175	4.3128	5.7349	9.7009	10.258
$6 \times 12 \times 2$	432	1.0512	4.2155	4.3109	5.7345	9.6970	10.254
$7 \times 14 \times 3$	882	1.0508	4.2135	4.3088	5.7340	9.6913	10.248
Liew et al. (1994)	1365[a]	1.0594	4.2856	4.3685	5.7399	10.067	10.700

[a] A half of the size (2730) of the actual determinant in Liew's paper because that the symmetry of the plate in the ξ direction is not considered in their paper.

Table 3
The comparison study of eigenfrequencies for cantilevered isosceles triangular plates with different thickness-to-width ratio and apex angles using three-dimensional elasticity theory and Mindlin plate theory, respectively

Reference	γ	λ_1^{AS}	λ_2^{AS}	λ_3^{AA}	λ_4^{AS}	λ_5^{AA}	λ_6^{AS}
$\alpha = 30°$							
Kitipornchai et al. (1993)	0.05	0.3133	1.350	2.081	3.260	5.102	5.979
Present[a]		0.3137	1.351	2.084	3.265	5.109	5.989
Kitipornchai et al. (1993)	0.1	0.3115	1.326	1.980	3.148	4.725	5.647
Present[b]		0.3121	1.329	1.985	3.158	4.742	5.670
Kitipornchai et al. (1993)	0.2	0.3062	1.251	1.709	2.820	3.801	4.780
Present[c]		0.3072	1.257	1.717	2.840	3.826	4.825
$\alpha = 60°$							
Kitipornchai et al. (1993)	0.05	1.404	5.387	5.929	13.50	13.86	15.99
Present[d]		1.407	5.399	5.944	13.54	13.90	16.04
Kitipornchai et al. (1993)	0.1	1.376	4.999	5.540	12.00	12.12	13.85
Present[e]		1.380	5.023	5.569	12.20	12.09	13.96
Kitipornchai et al. (1993)	0.2	1.295	4.051	4.586	8.802	9.060	10.06
Present[f]		1.303	4.087	4.636	8.908	9.182	10.21
$\alpha = 90°$							
Kitipornchai et al. (1993)	0.05	3.926	10.84	15.58	24.36	27.26	36.03
Present[g]		3.938	10.88	15.65	24.49	27.41	36.26
Kitipornchai et al. (1993)	0.1	3.741	9.661	13.41	20.11	22.19	27.96
Present[h]		3.762	9.734	13.53	20.33	22.42	28.31
Kitipornchai et al. (1993)	0.2	3.267	7.250	9.583	13.65	14.81	17.85
Present[i]		3.300	7.347	9.743	13.90	15.06	18.19

[a] Additional SA mode presented by the three-dimensional Ritz solution is 4.111.
[b] Additional SA modes presented by the three-dimensional Ritz solution are 2.057 and 4.999.
[c] Additional SA modes presented by the three-dimensional Ritz solution are 1.029; 2.501 and 4.294 and SS mode is 3.346.
[d] Additional SA mode presented by the three-dimensional Ritz solution is 14.099.
[e] Additional SA mode presented by the three-dimensional Ritz solution is 7.054 and SS mode is 13.77.
[f] Additional SA modes presented by the three-dimensional Ritz solution are 3.531 and 7.056 and SS mode is 6.895.
[g] Additional SA mode presented by the three-dimensional Ritz solution is 2.798.
[h] Additional SA modes presented by the three-dimensional Ritz solution are 14.00 and 25.42 and SS mode is 22.40.
[i] Additional SA modes presented by the three-dimensional Ritz solution are 7.006 and 12.70 and SS modes are 11.22 and 18.05.

$$\lambda = (\omega a^2/2\pi)\sqrt{\rho t/D} = \Omega\sqrt{12(1-\nu^2)}/(2\pi\gamma). \tag{20}$$

In all the computation, the Poisson's ratio ν is assumed to be 0.3. Equal numbers of Chebyshev polynomial series are taken for U, V and W in Eq. (11) in each direction, i.e. $I = L = P$, $J = M = Q$ and $K = N = R$,

although in most cases, computational optimization could be obtained by using unequal numbers of series terms. Taking into account the asymmetry of the plates in the η direction, the numbers of the Chebyshev polynomials used in the η direction are double of those used in the ξ direction. From Table 1, it is observed that the present three-dimensional Ritz solutions converge monotonically from the above to the eigenfrequency values with the increase of the number of terms of the Chebyshev polynomial series. Moreover, it is shown that the rate of convergence for the first six eigenfrequencies is more sensitive to the orders I and J of the Chebyshev series employed in the surface function (ξ–η plane) than the order K of the series employed in the thickness direction (ζ direction). However, with the increase of the thickness-to-width ratio, more terms of Chebyshev polynomials in the ζ direction accompanying less terms used in the ξ–η plane are needed. It is further seen that for the plate with thickness-to-width ratio $\gamma = 0.05$, the first six eigenfrequencies converge to five-digit accuracy using $8 \times 16 \times 2$ terms of the Chebyshev polynomials. For $\gamma = 0.15$ the first six eigenfrequencies converge to five-digit accuracy using $6 \times 12 \times 3$ terms of the Chebyshev polynomials. And for $\gamma = 0.45$ the first six eigenfrequencies converge to five-digit accuracy using $5 \times 10 \times 4$ terms of the Chebyshev polynomials. In Table 2, the convergence and accuracy of the first six eigenfrequencies for the cantilevered isosceles triangular plate with thickness-to-width ratio $\gamma = 0.1$ and apex angle $\alpha = 53.13°$ are validated through comparison with the results presented by Liew et al. (1994). Up to now, Liew's results are the only available data for isosceles triangular plates using three-dimensional elasticity theory in literature. In Liew's paper, one- and two-dimensional orthogonal polynomial functions are developed as the admissible functions of each displacement component in the Ritz method. It is shown that using Chebyshev polynomials as the admissible functions can give higher accuracy and more rapid convergence than using orthogonal polynomials. The eigenfrequencies for cantilevered isosceles triangular plates with moderate thickness are presented in Table 3 together with the Mindlin plate solutions presented by Kitipornchai et al. (1993). Three different thickness-to-width ratios $\gamma = 0.05$, $\gamma = 0.1$ and $\gamma = 0.2$ as well

Table 4
The comparison study of eigenfrequencies for isosceles triangular plates with small apex angles $\alpha = 2\tan^{-1}(t/2l)$, respectively, using three-dimensional elasticity theory and Timoshenko beam theory

t/l	Theories	$\tilde{\lambda}_1^{SA}$	$\tilde{\lambda}_2^{SA}$	$\tilde{\lambda}_3^{SA}$	$\tilde{\lambda}_1^{AS}$	$\tilde{\lambda}_2^{AS}$	$\tilde{\lambda}_3^{AS}$
0.04	3-D	5.3167	15.194	29.955	7.1447	30.780	73.910
	T-Beam[a]	5.3099	15.172	29.897	7.1404	30.713	73.730
0.1	3-D	5.3003	15.059	29.483	7.0841	29.289	66.725
	T-Beam	5.2830	14.992	29.279	7.0579	29.161	66.362
0.15	3-D	5.2781	14.852	28.739	6.9723	27.418	59.307
	T-Beam	5.2438	14.735	28.430	6.9412	27.261	58.870
0.2	3-D	5.2410	14.563	27.766	6.8199	25.327	52.339
	T-Beam	5.1902	14.398	27.364	6.7887	25.163	51.889
0.25	3-D	5.1932	14.208	26.627	6.6370	23.246	46.341
	T-Beam	5.1235	13.996	26.166	6.6088	23.086	45.908
0.3	3-D	5.1356	13.799	25.388	6.4336	21.297	41.330
	T-Beam	5.0453	13.548	24.914	6.4098	21.145	40.929
0.35	3-D	5.0673	13.350	24.115	6.2156	19.523	37.162
	T-Beam	4.9573	13.072	23.666	6.1992	19.387	36.806
0.4	3-D	4.9920	12.875	22.850	5.9909	17.938	33.679
	T-Beam	4.8610	12.582	22.463	5.9830	17.819	33.373

[a] The results using Timoshenko beam theory come from Zhou and Cheung (2001).

as three different apex angles $\alpha = 30°$, $\alpha = 60°$ and $\alpha = 90°$ are considered. It is shownthat Mindlin plate theory presents lower eigenfrequencies when a shear correction factor $\kappa = 5/6$ is used and the differences between the three-dimensional elasticity solutions and the Mindlin plate solutions increase with the increase of thickness-to-width of the plates. Moreover, it should be noticed that the three-dimensional elasticity theory is able to represent more vibration modes than the Mindlin plate theory because the Mindlin plate theory ignores the effect of symmetric deformation in the thickness direction of the plates. Therefore, the SA and SS modes cannot be presented by the Mindlin plate theory, as seen from Table 3. It is obvious that for a small apex angle, the plate can be approximately considered as a beam. In such a case, the results from the exact three-dimensional elasticity theory should tend to approach the solutions of the one-dimensional beam theory. A comparison of eigenfrequency parameters for cantilevered isosceles triangular plates with small apex angles, resulted from the exact three-dimensional elasticity theory (3-D) and the Timoshenko beam theory (T-Beam) (Zhou and Cheung, 2001) is given in Table 4 for a plate with a square larger end ($\gamma = 1.0$). A new eigenfrequencies parameter $\tilde{\lambda}$ is defined as $\tilde{\lambda} = \omega l^2(\rho A_0/EI_0)^{1/2} = \Omega(12)^{1/2}/(t/l)^2$ where A_0 and I_0 are, respectively, the cross-sectional area and the area moment of inertia of the plate at the larger end

Table 5
The eigenfrequencies of AS modes for cantilevered isosceles triangular plates with respect to different thickness-to-width ratios γ and apex angles α

γ	λ_1	λ_2	λ_3	λ_4	λ_5	λ_6
$\alpha = 30°$						
0.1	0.31208	1.3290	3.1578	5.6701	8.4482	8.8130
0.2	0.30716	1.2572	2.8394	4.8242	6.8130	7.0857
0.3	0.30065	1.1652	2.4918	4.0363	5.5084	5.7025
0.4	0.29274	1.0674	2.1797	3.4103	4.5622	4.7017
0.5	0.28387	0.97324	1.9187	2.9357	3.8671	3.9656
$\alpha = 60°$						
0.1	1.3804	5.5686	12.088	13.965	20.466	24.298
0.2	1.3030	4.6361	9.1827	10.207	14.221	16.452
0.3	1.2087	3.8016	7.1440	7.7788	10.399	11.971
0.4	1.1112	3.1552	5.7801	6.2136	7.4208	8.8431
0.5	1.0193	2.6682	4.8082	5.1032	5.4213	7.1192
$\alpha = 90°$						
0.1	3.7621	13.531	20.326	28.311	34.951	44.830
0.2	3.3011	9.7465	13.902	18.199	21.947	26.158
0.3	2.8442	7.2894	10.203	13.101	14.210	16.597
0.4	2.4598	5.7209	7.9228	9.6688	10.154	11.841
0.5	2.1431	4.6566	6.3490	7.3325	8.1635	9.0187
$\alpha = 120°$						
0.1	9.4729	26.079	35.378	45.454	57.624	66.163
0.2	7.3914	16.948	20.965	27.171	31.719	35.002
0.3	5.8426	12.118	14.343	18.638	19.360	21.281
0.4	4.7629	9.2836	10.776	13.230	14.068	15.081
0.5	3.9935	7.4590	8.5962	10.029	10.591	11.786
$\alpha = 150°$						
0.1	29.538	52.443	73.125	81.662	96.136	110.97
0.2	18.946	31.021	39.388	42.087	45.547	51.587
0.3	13.600	21.709	25.555	27.062	29.323	31.860
0.4	10.535	16.626	18.605	19.141	21.393	22.239
0.5	8.5811	13.387	14.047	14.960	16.358	17.192

and l is the length of the plate. It is shown that with the decrease of the thickness-to-length ratio t/l $[\alpha = 2\tan^{-1}(t/2l)]$, the SA modes of the three-dimensional plates are close to the modes of the one-dimensional beams with linearly varying thickness. While the AS modes of the three-dimensional plates are close to the modes of the one-dimensional beams with linearly varying width.

4. Numerical results

Having confirmed its rapid convergence and high accuracy, the present formulation is applied to the computation of the non-dimensional eigenfrequency parameters λ for cantilevered and completely free isosceles triangular plates. The effect of thickness-to-width ratios γ and apex angles α is investigated in detail. Five thickness-to-width ratios from 0.1 to 0.5 with an increment of 0.1 and five apex angles from 30° to 150° with an increment of 30° are considered. The first six eigenfrequency parameters of AS and SA modes and the first three eigenfrequency parameters of SA and SS modes are given in Tables 5–10,

Table 6
The eigenfrequencies of AA modes for cantilevered isosceles triangular plates with respect to different thickness-to-width ratios γ and apex angles α

γ	λ_1	λ_2	λ_3	λ_4	λ_5	λ_6
$\alpha = 30°$						
0.1	1.9848	4.7414	7.9106	11.459	15.284	16.336
0.2	1.7170	3.8249	5.9403	7.9957	9.9428	11.800
0.3	1.4292	2.9414	4.2167	5.4087	6.7063	8.0894
0.4	1.1681	2.2044	3.0514	3.9858	4.9902	6.0294
0.5	0.94935	1.6670	2.3466	3.1190	3.9284	4.5771
$\alpha = 60°$						
0.1	5.0226	12.201	20.242	23.411	29.482	35.194
0.2	4.0872	8.9082	13.519	15.599	18.051	21.279
0.3	3.2383	6.5316	9.0877	10.719	11.649	13.172
0.4	2.5690	4.8211	6.4878	7.4204	8.1521	9.1323
0.5	2.0597	3.6459	4.9906	5.5058	6.1309	7.0885
$\alpha = 90°$						
0.1	9.7339	22.421	31.697	38.082	46.650	55.443
0.2	7.3493	15.061	19.904	22.265	26.704	28.413
0.3	5.5661	10.702	12.771	13.086	16.109	17.093
0.4	4.3191	7.5204	8.8238	9.2127	11.776	12.298
0.5	3.4362	5.5670	6.5609	7.4277	9.1630	9.3755
$\alpha = 120°$						
0.1	18.280	35.741	50.273	55.788	69.062	76.864
0.2	12.538	22.535	27.352	29.164	32.573	36.401
0.3	9.0969	14.727	16.247	17.213	22.094	22.662
0.4	6.9354	9.7969	12.061	12.603	15.755	16.388
0.5	5.4920	7.3737	9.2821	10.256	11.366	12.393
$\alpha = 150°$						
0.1	41.887	63.559	84.502	99.368	107.59	114.68
0.2	25.173	36.404	36.971	45.281	47.660	51.949
0.3	17.440	20.951	25.689	28.616	31.400	33.221
0.4	13.061	14.907	19.496	20.382	21.729	23.022
0.5	10.321	11.690	14.697	15.722	16.436	17.550

Table 7
The eigenfrequencies of SA and SS modes for cantilevered isosceles triangular plates with respect to different thickness-to-width ratios γ and apex angles α

γ	λ_1^{SA}	λ_2^{SA}	λ_3^{SA}	λ_1^{SS}	λ_2^{SS}	λ_3^{SS}
$\alpha = 30°$						
0.1	2.0566	4.9994	8.5869	6.6868	15.223	22.349
0.2	1.0291	2.5008	4.2941	3.3461	7.6123	11.167
0.3	0.68668	1.6681	2.8639	2.2323	5.0723	7.4301
0.4	0.51540	1.2518	2.1492	1.6751	3.7991	5.5490
0.5	0.41264	1.0022	1.7206	1.3406	3.0322	4.4041
$\alpha = 60°$						
0.1	7.0541	14.114	23.644	13.772	28.325	31.265
0.2	3.5314	7.0560	11.812	6.8955	14.145	15.605
0.3	2.3569	4.7028	7.8626	4.6006	9.3874	10.355
0.4	1.7697	3.5257	5.8799	3.4514	6.9696	7.6613
0.5	1.4173	2.8188	4.6589	2.7601	5.4377	5.8103
$\alpha = 90°$						
0.1	13.996	25.423	40.305	22.401	36.213	43.939
0.2	7.0060	12.704	20.147	11.219	18.049	21.864
0.3	4.6752	8.4529	13.419	7.4802	11.915	14.277
0.4	3.5099	6.3140	9.2812	5.6019	8.7183	9.4591
0.5	2.8109	5.0049	6.2189	4.4626	6.3045	6.6247
$\alpha = 120°$						
0.1	24.492	42.103	57.382	36.126	47.949	57.822
0.2	12.254	20.996	28.597	18.085	23.890	28.631
0.3	8.1739	13.821	17.821	12.013	15.493	17.271
0.4	6.1352	9.8951	11.457	8.8496	10.434	11.519
0.5	4.9129	7.2394	8.7076	6.6575	7.7102	8.7016
$\alpha = 150°$						
0.1	49.180	80.935	90.086	71.542	75.457	94.430
0.2	24.585	38.379	43.522	35.425	36.435	42.899
0.3	16.393	22.035	27.418	20.369	24.087	25.258
0.4	12.304	15.016	18.424	13.570	17.778	18.130
0.5	9.8548	11.382	13.540	10.129	13.891	14.492

Table 8
The eigenfrequencies of AS modes for completely free isosceles triangular plates with respect to different thickness-to-width ratios γ and apex angles α

γ	λ_1	λ_2	λ_3	λ_4	λ_5	λ_6
$\alpha = 30°$						
0.1	1.2263	3.0564	4.5810	5.6261	8.7328	9.6395
0.2	1.1776	2.7964	4.0343	4.8893	7.1892	7.8109
0.3	1.1143	2.4992	3.4879	4.1676	5.8633	6.3541
0.4	1.0447	2.2169	3.0204	3.5650	4.8249	5.2795
0.5	0.97491	1.9651	2.6351	3.0768	3.9295	4.3690
$\alpha = 60°$						
0.1	5.1220	5.2164	11.674	15.352	20.024	20.493
0.2	4.4435	4.5198	9.0950	11.691	13.511	14.792
0.3	3.7275	3.9210	6.9974	8.9910	9.1722	11.075
0.4	3.1369	3.4139	5.3153	6.1282	7.4608	7.6839
0.5	2.6582	3.0018	4.0817	4.4547	5.8304	6.1936

Table 8 (*continued*)

γ	λ_1	λ_2	λ_3	λ_4	λ_5	λ_6
$\alpha = 90°$						
0.1	5.5685	12.005	18.791	22.848	29.158	33.756
0.2	4.7666	8.9381	13.454	13.984	18.634	20.173
0.3	4.0050	6.4225	8.5548	10.508	11.855	12.930
0.4	3.3608	4.6045	6.3498	7.7538	8.5291	8.9076
0.5	2.8118	3.5268	5.0493	5.7671	6.6541	6.7823
$\alpha = 120°$						
0.1	5.8244	17.595	22.754	32.789	38.114	42.855
0.2	4.9086	9.9887	13.405	15.924	21.126	24.091
0.3	4.0689	5.5646	9.1534	10.530	13.641	14.916
0.4	3.2330	3.8764	6.4791	8.0773	8.4760	9.6745
0.5	2.4438	3.2146	4.9337	5.4932	6.3294	7.3394
$\alpha = 150°$						
0.1	5.8239	18.727	19.839	28.394	37.099	40.435
0.2	4.8523	6.1210	10.320	14.245	15.888	19.358
0.3	3.0357	4.2381	5.8475	8.2711	9.4814	10.892
0.4	1.9347	3.5770	4.0545	4.6750	6.7064	7.6823
0.5	1.3859	2.8600	3.0445	3.3070	4.8743	5.1312

respectively. For $\gamma = 0.1$ and $\gamma = 0.2$, $7 \times 14 \times 3$ terms of Chebyshev polynomials; for $\gamma = 0.3$ and $\gamma = 0.4$, $6 \times 12 \times 4$ terms and for $\gamma = 0.5$, $6 \times 12 \times 5$ terms are used in the computation. It is seen that with the increase of the plate thickness, eigenfrequencies will monotonically decrease for the cantilevered isosceles triangular plates. While the eigenfrequencies monotonically increase with the increase of the apex angle. Such a phenomenon cannot be observed for the completely free isosceles triangular plates.

5. Concluding remarks

In this paper, a global three-dimensional Ritz formulation is presented for the free vibration analysis of cantilevered and completely free isosceles triangular plates. The triangular plate domain is mapped onto a basic cubic domain and a set of Chebyshev polynomial series multiplying by a boundary function is developed as the admissible functions of each displacement component. High accuracy and low computational cost are confirmed by the convergence and comparison studies. In the analysis, an exact three-dimensional elasticity theory based on isotropic material and small strain is used. Extensive and accurate eigenfrequencies are reported for the free vibration of completely free isosceles triangular plates for the first time in literature. Although other numerical methods such as finite element methods and finite difference methods can also be applied to solve the problem considered here, they typically require many more degrees of freedom. This necessarily results in the evaluation of much larger sizes of eigenfrequency equation to achieve satisfactory results, resulting in greater cost in a computation. The data from the present Ritz solutions can be used as standard to judge the accuracy of other numerical methods and various kinds of two-dimensional plate theories and one-dimensional beam theories. Moreover, it is seen that higher accuracy, more rapid convergence as well as better numerical stability in the computation can be obtained by using the Chebyshev polynomial series as the admissible functions than using other polynomial series. In future research, it would be fruitful to develop further the potential of Chebyshev polynomials in the three-dimensional vibration analysis of other structural elements with different geometric shapes.

Table 9
The eigenfrequencies of AA modes for completely free isosceles triangular plates with respect to different thickness-to-width ratios γ and apex angles α

γ	λ_1	λ_2	λ_3	λ_4	λ_5	λ_6
$\alpha = 30°$						
0.1	2.5164	5.0007	8.0621	10.705	11.625	15.470
0.2	2.2124	4.0949	6.1296	8.1039	8.5184	10.149
0.3	1.8790	3.1928	4.3733	5.5343	6.4822	6.9642
0.4	1.5522	2.4257	3.2078	4.0639	4.8101	5.2807
0.5	1.2531	1.8821	2.5145	3.0945	3.6237	4.0872
$\alpha = 60°$						
0.1	5.2164	11.674	12.049	20.024	25.333	29.065
0.2	4.4435	8.7562	9.0950	13.511	17.219	17.243
0.3	3.7275	6.0873	6.9974	8.9010	10.489	11.634
0.4	3.1369	4.1290	5.3153	6.1282	7.2194	7.6839
0.5	2.6582	2.8620	4.0817	4.4547	5.3909	5.8304
$\alpha = 90°$						
0.1	8.2027	12.951	20.243	28.751	33.058	40.602
0.2	6.6076	9.2433	13.197	16.888	19.645	22.735
0.3	4.9871	6.5272	8.7245	10.098	12.772	13.277
0.4	3.4757	5.0966	6.1577	6.5197	8.4843	9.1997
0.5	2.4365	4.1577	4.5573	4.7036	6.4373	6.9829
$\alpha = 120°$						
0.1	10.612	15.427	25.868	31.243	41.216	46.444
0.2	7.7169	9.0138	13.088	17.794	19.875	24.969
0.3	4.3199	7.0419	7.6288	11.250	12.148	14.226
0.4	2.6733	4.9697	5.9657	7.0382	8.1549	8.7164
0.5	1.8053	3.6723	4.6765	5.2092	5.4069	6.4842
$\alpha = 150°$						
0.1	11.590	15.665	24.004	28.011	34.733	46.524
0.2	5.0585	8.3559	9.3877	13.212	18.700	19.771
0.3	2.4682	4.4870	7.4973	7.6311	8.4809	11.516
0.4	1.4686	2.9275	4.6194	5.3085	6.2018	7.3320
0.5	0.97457	2.1370	2.9750	4.0444	4.7539	4.9035

Table 10
The eigenfrequencies of SA and SS modes for completely free isosceles triangular plates with respect to different thickness-to-width ratios γ and apex angles α

γ	λ_1^{SA}	λ_2^{SA}	λ_3^{SA}	λ_1^{SS}	λ_2^{SS}	λ_3^{SS}
$\alpha = 30°$						
0.1	4.5385	8.6799	12.824	10.445	14.825	18.216
0.2	2.2691	4.3397	6.4117	5.2202	7.4070	9.1044
0.3	1.5127	2.8935	4.2754	3.4777	4.9314	6.0650
0.4	1.1346	2.1710	3.2075	2.6055	3.6909	4.5432
0.5	0.90780	1.7377	2.5657	2.0814	2.9438	3.6275
$\alpha = 60°$						
0.1	13.725	20.383	22.112	13.725	20.383	23.373
0.2	6.8578	10.188	11.041	6.8578	10.188	11.645
0.3	4.5667	6.7890	7.3461	4.5667	6.7890	7.7102
0.4	3.4193	5.0880	5.4935	3.4193	5.0880	5.7118
0.5	2.7287	4.0652	4.3681	2.7287	4.0652	4.4686

Table 10 (*continued*)

γ	λ_1^{SA}	λ_2^{SA}	λ_3^{SA}	λ_1^{SS}	λ_2^{SS}	λ_3^{SS}
$\alpha = 90°$						
0.1	18.083	26.494	31.519	12.084	22.847	27.656
0.2	9.0349	13.225	15.737	6.0396	11.407	13.809
0.3	6.0178	8.7858	10.452	4.0244	7.5846	9.1799
0.4	4.5057	6.5352	7.0817	3.0160	5.6600	6.7375
0.5	3.5872	4.6295	5.0986	2.4087	4.4523	4.4933
$\alpha = 120°$						
0.1	14.622	29.162	35.905	9.2177	21.677	25.073
0.2	7.3163	14.611	17.852	4.6096	10.850	12.516
0.3	4.8854	9.4036	10.012	3.0740	7.2370	8.3053
0.4	3.6680	5.4246	7.3780	2.3049	5.2631	5.5549
0.5	2.9246	3.5327	5.4078	1.8403	3.3804	4.3213
$\alpha = 150°$						
0.1	8.2788	17.949	29.962	5.0655	13.122	23.568
0.2	4.1546	9.0378	12.089	2.5351	6.5998	11.707
0.3	2.7824	5.2964	6.1068	1.6916	4.4111	5.3307
0.4	2.0930	3.0014	4.5773	1.2684	2.9567	3.3515
0.5	1.6699	1.9470	3.3183	1.0122	1.8633	2.6291

Acknowledgements

The financial support from CRCG of the University of Hong Kong is gratefully acknowledged.

References

Batoz, J.L., Bathe, K.J., Ho, L.W., 1980. A study of three-node triangular plate bending element. Int. J. Numer. Meth. Engng. 15, 1771–1812.

Cox, H.L., Klein, B., 1995. Fundamental frequencies of clamped triangular plates. J. Acoust. Soc. Am. 27, 266–268.

Fox, L., Parker, I.B., 1968. Chebyshev Polynomials in Numerical Analysis. Oxford University Press, London.

Gorman, D.J., 1989a. Accurate free vibration analysis of right triangular plates with one free edges. J. Sound Vib. 131, 115–125.

Gorman, D.J., 1989b. Accurate analytical solution for free vibration of the simply supported triangular plate. AIAA J. 27, 647–651.

Karunasena, W., Kitipornchai, S., Al-Bermani, F.G.A., 1996. Free vibration of cantilevered arbitrary triangular Mindlin plates. Int. J. Mech. Sci. 38, 431–442.

Kim, C.S., Dickinson, S.M., 1990. The free flexural vibration of right triangular isotropic and orthotropic plates. J. Sound Vib. 141, 291–311.

Kitipornchai, S., Liew, K.M., Xiang, Y., Wang, C.M., 1993. Free vibration of isosceles triangular Mindlin plates. Int. J. Mech. Sci. 35, 89–102.

Lam, K.Y., Liew, K.M., Chow, S.T., 1990. Free vibration analysis of isotropic and orthotropic triangular plates. Int. J. Mech. Sci. 32, 455–464.

Liew, K.M., Hung, K.C., Lim, M.K., 1994. Three-dimensional elasticity solutions to vibration of cantilevered skewed trapezoids. AIAA J. 32, 2080–2089.

McGee, O.G., Butalia, T.S., 1992. Natural vibrations of shear deformable cantilevered skewed trapezoidal and triangular thickness plates. Comput. Struct. 45, 1033–1059.

McGee, O.G., Giaimo, G.T., 1992. Three-dimensional vibrations of cantilevered right triangular plates. J. Sound Vib. 159, 279–293.

Mindlin, R.D., 1951. Influence of rotary inertia and shear in flexural motion of isotropic elastic plates. ASME J. Appl. Mech. 18, 31–38.

Timoshenko, S.P., Woinowsky-Krieger, S., 1959. Theory of Plates and Shells. McGraw-Hill, New York.

Zhou, D., Cheung, Y.K., 2001. Vibration of tapered Timoshenko beams in terms of static Timoshenko beam functions, ASME J. Appl. Mech. 68, 596–602.